The Source of the Fine Structure Constant

Phineas Proffett (private researcher)

The dimensionless fine structure constant ($\alpha=e^2/4\pi\varepsilon_0\hbar c=0.0072973525643=1/137.035999177$) first reared its head in 1916 at a time when the scientific community visualized electrons orbiting the nucleus according to Niels Bohr's theory of hydrogen that he had proposed three years earlier. After physicists leapfrogged from orbital motion to probability density functions for electrons in 1926 with Erwin Schrödinger's equation, the fine-structure constant found application in a wide range of quantum phenomena. In the intervening century, physicists have been both fascinated and somewhat spooked by the fine structure constant because it determines the values of the crucial constants of physics that have allowed life to emerge in our universe- thus suggesting that there was conscious intent which predates the Big Bang that was behind the fine-tuning of these constants. Physicists more readily recognize the inverse of the fine structure constant: $1/\alpha= 137.035999177$. They have wondered what the source of this dimensionless value is- where does the number 137.035999177 come from? This paper proffers a novel derivation of the fine structure constant that is presumed to be the true source. This derivation suggests that leapfrogging from two-dimensional orbits for the electron to three-dimensional probability density functions missed a step that has eluded the scientific community. The missing step entails magnetic dipole interactions between the electron and the nucleus that forces elliptical orbits into spherical orbits. And rather than random positions for electrons, their orbits may be highly synchronized such that an atom operates more like a fine Swiss watch- at least when the probability function is collapsed in the manner of any wavefunction. The proposed source of the fine structure constant is $1/\alpha=\sqrt{f_e/f_L}$, where f_e is the rotation rate of the electron in the first Bohr orbit, and f_L is the Larmor precession rate of the electron in the first Bohr orbit. The g-factor of the electron must be set to 2, rather than the anomalous value of 2.00232, for this novel derivation to produce the precise value of $1/\alpha$. Thus, the orbital wavefunction and/or bound electron states may suppress the quantum effects that produce the anomalous value. The implication is that the fine structure constant is fine-tuned to allow electrons to achieve organized, repeatable orbitals so that predictable, determinate biomolecules may be constructed to permit life to emerge.

The Novel Derivation of $1/\alpha$

The derivation of the fine structure constant through this novel means will first be rendered, followed by a discussion of its import to the field of quantum physics. All the steps will be presented in minute detail with values inserted to ease the process of confirming the validity of this novel derivation. The values below will be used for the constants of physics. Note that $\hbar=h/2\pi$ without rounding to yield the 2022 CODATA value of 137.035999177 directly by calculating $1/\alpha = 4\pi\varepsilon_0\hbar c/e^2$.

$m_e = 9.1093837139 \times 10^{-31}$ kg
$e = 1.602176634 \times 10^{-19}$ C
$\varepsilon_0 = 8.8541878188 \times 10^{-12}$ F·m^{-1}
$\mu_0 = 1.25663706127 \times 10^{-6}$ N·A^{-2}
$\hbar = 1.05457181765 \times 10^{-34}$ J ·s
$c = 2.99792458 \times 10^{8}$ m·s^{-1}

To calculate the fine structure constant from the novel formula:

$$1/\alpha=\sqrt{f_e/f_L}, \quad (1)$$

the first step is to determine f_e- the rotation rate of the electron in the first Bohr orbit. This can be derived by dividing the velocity (V_e) of the electron in the first Bohr orbit by the circumference of this orbit ($2\pi r_e$). Niels Bohr derived the formulas for V_e and r_e that predate Schrödinger's equation by thirteen years:

$$r_e = \frac{4\pi\varepsilon_0\hbar^2}{m_e e^2} \quad (2)$$

$$= \frac{4\pi(8.8541878188 \text{ x } 10^{-12})(1.05457181765 \text{ x } 10^{-34})^2}{(9.1093837139 \text{ X } 10^{-31})(1.602176634 \text{ x } 10^{-19})^2}$$

$$r_e = 5.29177210548 \text{ x } 10^{-11} \text{ m}$$

$$V_e = \frac{1}{4\pi\varepsilon_0}\frac{e^2}{\hbar} \qquad (3)$$

$$= \frac{(1.602176634 \text{ x } 10^{-19})^2}{4\pi(8.8541878188 \text{ x } 10^{-12})(1.05457181765 \text{ x } 10^{-34})}$$

$$V_e = 2.18769126215 \text{ X } 10^6 \text{ m/s}$$

$$f_e = V_e/(2\pi\, r_e) \qquad (4)$$

$$= \frac{2.18769126215 \text{ X } 10^6}{2\pi(5.29177210548 \text{ x } 10^{-11})}$$

$$f_e = 6.57968392042 \text{ X } 10^{15}$$
(revolutions per second)

The next step is to derive the Larmor precession of the electron (f_L) in the first Bohr orbit. From the perspective of the hydrogen atom, the electron is orbiting a single proton, which will immerse the proton in a magnetic field. However, from the perspective of the electron, the single proton of the hydrogen atom appears to be orbiting around it, which immerses the electron in its magnetic field. The seemingly orbiting proton constitutes a current loop with the electron in the center of the loop. The magnetic field (B) in which the electron is immersed can be calculated from the Biot and Savart Law:

$$B = \frac{\mu_0 I r_e^2}{2(r_e^2 + Z^2)^{3/2}}.$$

Z is the distance along an axis that is encircled by a current loop. Since the electron is at the center of the current loop, Z can be set to zero. This simplifies the equation to:

$$B = \frac{\mu_0 I}{2r_e} \qquad (5)$$

Now the current I is due to the seemingly circulating proton charge (e=1eV=1.6 X 10^{-19} Coulombs), which amounts to the rate at which the charge is circulating in a loop. This current is:

$$I = ef_e = eV_e/(2\pi r_e) \qquad (6)$$

Substituting equation (6) into (5) produces:

$$B = \frac{\mu_0 e V_e}{4\pi r_e^2} \qquad (7)$$

$$= \frac{(1.25663706127 \text{ x } 10^{-6})(1.602176634 \text{ x } 10^{-19})(2.18769126215 \text{ X } 10^6)}{4\pi(5.29177210548 \text{ x } 10^{-11})^2}$$

$$B = 12.5168244296 \text{ T}$$

The Larmor precession for an electron immersed in a magnetic field B is:

$$\omega_L = \gamma B$$

where $\gamma = \frac{eg}{2m_e}$.

The constant 'g' is the gyromagnetic ratio between the electron's magnetic moment and its angular momentum. Experiments have shown that it is slightly higher than 2- around 2.00232. The great achievement of quantum electrodynamics is to ascribe the propensity of the electron to not only exchange photons that would render g=2, but to also undergo other, less frequent processes to provide a

theoretical basis for an incrementally higher value. The dominant alternate process is for the electron to emit and absorb its own photon. Another, rarer process is for such a reabsorbed photon to briefly undergo pair production. Setting g=2 is what results in the precise value of the fine structure constant in this derivation. Therefore, perhaps these other alternate processes are suppressed either as a result of the activation of the orbital wavefunction, or because of the bound state of the electron. Experiments to detect the magnetic dipole moment of the electron in order to determine the gyromagnetic ratio rely on external magnetic fields or photons that would be presumed to disrupt the wavefunction of the orbital so that the alternate processes are no longer suppressed. A measurement is being taken, which generally collapses the wavefunction; and the electron assumes two different aspects on either side of the measurement before and after wavefunction collapse. At 6.58 x 10^{15} revolutions per second for the electron, which is presumed to be masked by the wavefunction of the orbital, there may not be enough time or spatial stability for the odd emission followed by absorption of the same photon, or for pair production as the electron rapidly alters its position around the nucleus while its angular momentum is constrained to integer values of ħ.

Instead of radians per second (ω_L) for the Larmor precession, precessions per second (f_L) is the appropriate unit to correspond with the rotation rate per second of the electron in its orbit around the nucleus:

$$f_L = \frac{\omega_L}{2\pi} = \frac{\gamma B}{2\pi} = \frac{egB}{2m_e(2\pi)} \qquad (8)$$

$$= \frac{(1.602176634 \text{ x } 10^{-19})(2)(12.5168244296)}{(2)(9.1093837139 \text{ X } 10^{-31})(2\pi)}$$

$$f_L = 3.50377080602 \text{ x } 10^{11}$$

Finally, taking the square root of the quotient of equation (4) over equation (8) produces the inverse fine structure constant:

$$\sqrt{\frac{f_e}{f_L}} = \sqrt{\frac{6.57968392042 \text{ X } 10^{15}}{3.50377080602 \text{ x } 10^{11}}} = 137.035999177$$

It is now obvious that the square root of the ratio between the Larmor precession rate of the electron and its rotation rate in the first Bohr orbit produces the value derived from the formula for the fine structure constant:

$$\sqrt{\frac{f_e}{f_L}} = 137.035999177$$

$$1/\alpha = 4\pi\varepsilon_0\hbar c/e^2 = 137.035999177$$

It only remains to prove that this novel derivation of the fine structure constant is equivalent to its formula:

$$\sqrt{\frac{f_e}{f_L}} = 4\pi\varepsilon_0\hbar c/e^2 = 1/\alpha \qquad (9)$$

This will now be done with the same level of minute detail as the preceding derivation. Starting with equations (4) and (8):

$$f_e = V_e/(2\pi r_e),$$

$$f_L = \omega_L/2\pi$$

We have:

$$\sqrt{\frac{f_e}{f_L}} = \sqrt{\frac{V_{e/(2\pi\, re)}}{\omega_L/(2\pi)}} = \sqrt{\frac{V_{e/\, re}}{\omega_L}} \qquad (10)$$

With $\omega_L = \gamma B = \frac{egB}{2m_e}$, for which g=2 we have:

$$\omega_L = \frac{eB}{m_e}$$

From equation (7), $B = \frac{\mu_0 e V_e}{4\pi {r_e}^2}$, so that

$$\omega_L = \frac{e\left[\frac{\mu_0 e V_e}{4\pi {r_e}^2}\right]}{m_e} \qquad (11)$$

Substituting (11) into (10) produces:

$$\sqrt{\frac{f_e}{f_L}} = \sqrt{\frac{V_{e/(re)}}{\omega_L}} = \sqrt{\frac{V_{e/\,re}}{\left[\frac{e\left(\frac{\mu_0 e V_e}{4\pi {r_e}^2}\right)}{m_e}\right]}}$$

We can cancel V_e/r_e from the numerator and denominator:

$$\sqrt{\frac{\cancel{V_e}/\cancel{re}}{\left[\frac{e\left(\frac{\mu_0 e \cancel{V_e}}{4\pi \cancel{r_e}^2}\right)}{m_e}\right]}} = \sqrt{\frac{1}{\frac{e}{m_e}\left(\frac{\mu_0 e}{4\pi r_e}\right)}} = \sqrt{\frac{m_e 4\pi r_e}{\mu_0 e^2}}$$

Using equation (2) for r_e, we have:

$$\sqrt{\frac{m_e 4\pi[r_e]}{\mu_0 e^2}} = \sqrt{\frac{4\pi m_e\left[\frac{4\pi\varepsilon_0\hbar^2}{m_e e^2}\right]}{\mu_0 e^2}}$$

Cancelling m_e from the numerator and multiplying like terms gets us to:

$$\sqrt{\frac{4\pi\cancel{m_e}\left[\frac{4\pi\varepsilon_0\hbar^2}{\cancel{m_e}e^2}\right]}{\mu_0 e^2}} = \sqrt{\frac{16\pi^2\left[\frac{\varepsilon_0\hbar^2}{e^2}\right]}{\mu_0 e^2}} = \sqrt{\frac{16\pi^2\varepsilon_0\hbar^2}{\mu_0 e^4}}$$

Now the speed of light $c = \sqrt{\frac{1}{\mu_0\varepsilon_0}}$, so

$$\mu_0 = 1/(\varepsilon_0 c^2)$$

Substituting for μ_0 in the previous equation produces:

$$\sqrt{\frac{16\pi^2\varepsilon_0\hbar^2}{(\mu_0)e^4}} = \sqrt{\frac{16\pi^2\varepsilon_0\hbar^2}{\left(\frac{1}{\varepsilon_0 c^2}\right)e^4}}$$

$$= \sqrt{\frac{16\pi^2{\varepsilon_0}^2\hbar^2 c^2}{e^4}} = \frac{4\pi\varepsilon_0\hbar c}{e^2} = \frac{1}{\alpha}$$

Thus: $\sqrt{\frac{f_e}{f_L}} = \frac{4\pi\varepsilon_0\hbar c}{e^2} = \frac{1}{\alpha}$,

where $1/\alpha$= 137.035999177- the inverse fine structure constant.

Influence of Precession on 1s Orbitals

Does this proposed source of the fine structure constant bring spin precession into play as an overlooked mechanism for determining atomic orbitals? Until 1926, when Erwin Schrödinger developed his famous wavefunction equation, electron orbits around the nuclei of atoms were visualized as being circular or elliptical- like planetary

orbits. This was a natural assumption arising from the fact that the electrostatic force matched the centripetal force of an orbiting electron, in analogy with the gravitational force matching the centripetal force of orbiting planets around the sun:

$$F = \frac{1}{4\pi\varepsilon_o}\frac{q_1 q_2}{r^2} \text{ (Electrostatic force)}$$

$$= \frac{1}{4\pi(8.8541878188\ \text{X}\ 10^{-12})}\frac{(1.602176634\ \text{X}\ 10^{-19})^2}{(5.29177210548\ \text{X}\ 10^{-10})^2}$$

$$= 8.2387235037 \text{ x } 10^{-8} \text{ N}$$

(Electrostatic attraction between an electron and proton in Hydrogen atom)

$$F = ma = \frac{mv^2}{r} \text{ (Centripetal Force)}$$

$$= \frac{(9.1093837139\ \text{X}\ 10^{-31})(2.18769126215\ \text{X}10^{6})^2}{5.29177210548\ \text{X}10^{-11}}$$

$$= 8.2387235037 \text{ x } 10^{-8} \text{ N}$$

(Centripetal force experienced by orbiting electron)

Electrons (as well as other quantum particles) were also thought to have a wavelength as they travelled due to de Broglie's equation that was promulgated in 1924. But shortly after Schrödinger published his famous equation two years later, the wavelength was interpreted as the probability amplitude of the electron. In 1913, Neils Bohr had explained why the electron does not spiral into the nucleus by confining the electron only to certain discrete energy levels through the energy equation he developed:

$$E_n = -\left[\frac{m_e}{2\hbar^2}\left(\frac{e^2}{4\pi\epsilon_0}\right)^2\right]\frac{1}{n^2} \qquad (12)$$

where (n)= 1,2, 3,....

Schrödinger's equation also produces this formula, which nowadays is viewed as the correct path to deriving it, whereas Bohr's derivation has been downgraded as having led to the correct solution more or less through dumb luck. For example, the third edition of *Introduction to Quantum Mechanics*, by David Griffiths, describes Bohr's

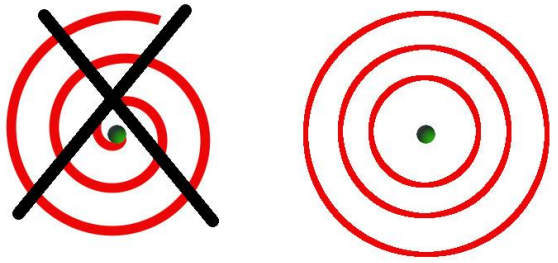

1913: Neils Bohr explained why electrons do not spiral into the nucleus- they are locked into discrete energy states.

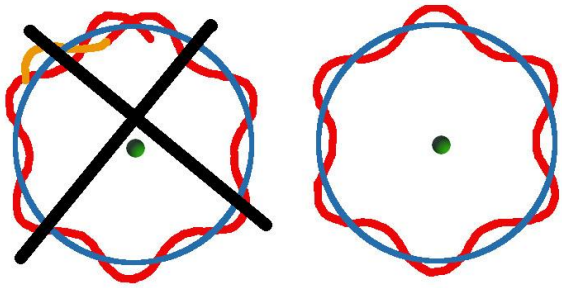

1924: De Broglie explained why the electron has discrete energy states in an atom- they must have an integral number of wavelengths that fit into its orbit around the nucleus. This wavelength fixes the electron's energy. So far we have only circular orbits in 2 dimensions.

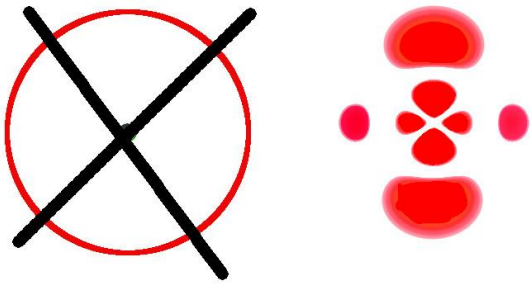

1926: Erwin Schrödinger leapfrogs from 2 dimensional circular orbits to 3 dimensional orbitals. Wavelengths are defined as probability amplitudes.

FIG. 1. Key milestones in quantum theory tracing the transition from visualizing two-dimensional elliptical electron orbits to imagining three-dimensional orbitals.

derivation as a "serendipitous mixture of inapplicable classical physics and premature quantum theory." The "inapplicable classical physics" refers mainly to Bohr's heavy reliance on the equivalence between the electrostatic force and the centripetal force of an orbiting electron to generate his equation. But a century ago, Bohr's equation that relied on the balance between these two forces was the gold standard that Schrödinger's equation had to cough up as a bewildering array of arcane solutions to integrals, truncated power series, mathematical assumptions and substitutions were thrown at it.

When the right combination reproduced equation (12), a radial wave function first had to be kneaded into the form below that preceded the final result:

$$\frac{d^2u}{d\rho^2} = \left[1 - \frac{\rho_0}{\rho} + \frac{\ell(\ell+1)}{\rho^2}\right] u. \qquad (13)$$

The only variables of interests in this discussion are ρ, which is a function of distance from the nucleus, and ℓ, which is the orbital angular momentum quantum number. The magnitude of the orbital angular momentum is $L=\sqrt{\ell(\ell+1)}\hbar$. ℓ also determines the shape of the orbital, which is spherical for ℓ=0 (the s shell), and has no angular momentum ($\sqrt{0(0+1)}=0$). ℓ=1 (the p shell) has two lobes, with an angular momentum of $\sqrt{1(1+1)}\hbar=\sqrt{2}\hbar$. ℓ=2 (the d shell) has an angular momentum of $\sqrt{2(2+1)}\hbar=\sqrt{6}\hbar$, and can have two or more lobes- the diagram on the bottom right in Fig. 1 is an example of the d shell.

It is in trying to make headway from equation (13) by making clever substitutions and manipulating a power series that quantum mechanics leapfrogged from two-dimensional elliptical orbits for the electron to three-dimensional orbitals; and in the process, skipped over the step that the proposed source of the fine structure constant has brought to light that reveals the mechanism through which elliptical orbits become three-dimensional. The precise operation on the equation at which this step is skipped is when ρ is made to approach zero so that the first and middle terms in parenthesis can be eliminated. The third term then dominates, which, after a series of ingenious mathematical manipulations, allows solutions of equation (13) to be used to resolve terms that had been establishing to knead the form of that equation into shape, which then readily reproduced Bohr's landmark equation (12). Since ρ is a function of distance from the nucleus, taking it to zero is presumed to be valid for the extremely small distances involved in atoms. But this is not valid for the s shell where ℓ=0 because the numerator of the third term ℓ(ℓ+1) is then zero, and the second term would dominate. So, the mechanism that transforms a circular orbit for the electron, which has orbital angular momentum, to the spherical s shell, which has no orbital angular momentum, is glossed over. Furthermore, this paper proposes that by glossing over this mechanism, all other orbitals generated by Schrödinger's equation require modification.

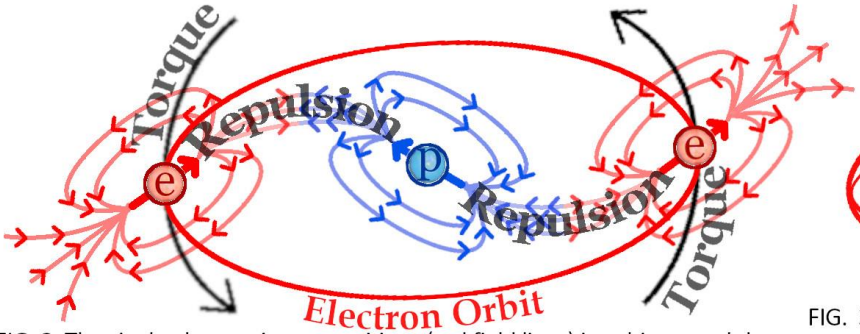

FIG. 2. The single electron in two positions (red field lines) in orbit around the proton (blue field lines) of the hydrogen atom. They are oriented at 55 degrees due to the internal magnetic fields of the atom inducing precession on their magnetic dipole moments. The field lines of the proton and electron exert a torque on the elliptical orbit of the electron- thus changing it into a spherical orbit. It is for this reason that the s shells exhibit no angular momentum- it is smeared out to zero as the elliptical orbit becomes spherical. The lines of torque are for clarity- the actual torque on the electron orbit points out of the page. If the electron is circulating clockwise, its angular momentum vector points downward, and the applied torque would "lift" the orbit as shown in Fig 3.

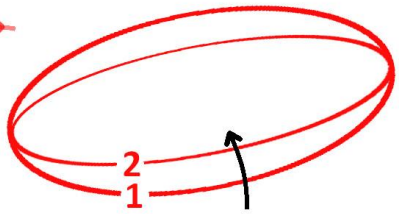

FIG. 3. The elliptical orbit of an electron constantly being torqued into spherical orbits. After around 2 million orbits, .35 ns have elapsed, and the orbital plane of the electron has changed by around 10 degrees from position '1' to '2'. The electron spin has precessed around 120 rotations in this proposed scenario, while the proton spin has precessed only around 66 degrees. A spherical shell will be traced out after around 12.5 ns, which smears the orbital angular momentum out to zero.

The proposed source of the fine structure constant implies that electron precession is the mechanism that forces the electron into spherical orbits for the s shell. Fig. 2 freezes the dipole moments of the single proton of the hydrogen atom and the single orbiting electron for the s shell at two instants of time- one with the electron having completed a half orbit on the left, and the other with it completing its full orbit on the right. Since the dipole moments of the electron and the proton are both directed upwards, there will always be repulsion between them in this orbit, regardless of the orientation of their dipole axes while they are precessing. There will be a downward component of repulsion during the left half of the orbit, and an upward component during the right half of the orbit. This will exert a torque on the axis of the elliptical orbit of the electron that will shift it after many orbits, as shown in Fig. 3. During this time, the axis of the electron's magnetic dipole moment has precessed though many complete rotations. The axis of the proton's magnetic dipole moment has precessed far less by a factor of 658, owing to the proton's greater mass and higher g-factor than the electron, according to Equation 8, or, equivalently, by the ratio between their dipole moments d_e and d_p, that will be encountered shortly. If the dipole moment of the proton were reversed, there would still be torque on the electron orbit, only the downward and upward forces would then be attractive.

The spin axes of the electron and proton in Fig. 2 are tilted at 55° while they are precessing in the presence of their mutually induced magnetic fields. This tilt θ can be determined from the magnitude of their spin angular momentum $\sqrt{s(s+1)}\hbar$, and the magnitude sħ that is projected along the direction of an external magnetic field, as measured in our three-dimensional universe, where s= ½. Thus:

$$\theta = \arccos \frac{1/2\,\hbar}{\sqrt{3}/2\,\hbar} = \arccos 1/\sqrt{3} = 54.7356^{o}$$

It requires complex modelling to show how spherical shells are being traced out by the axis of elliptical orbits constantly being shifted while the electron and proton are precessing. A very rough analysis based on the orientations shown in Fig. 3 will be undertaken here that should suffice to show that this mechanism of inducing spherical shells is viable. The analysis simply calculates the force between two magnetic dipoles placed end to end, and reduces it by a factor of ten- that will then be taken to be the average downward (or upward) force exerted on the electron orbit in Fig. 3. The formula below for point dipoles placed end to end may be used to calculate this force:

$$F = \frac{3\mu_0 d_e d_p}{2\pi r^4},$$

where:
$\mu_0 = 1.257 \times 10^{-6}$ N·A^{-2}
$d_e = 9.285 \times 10^{-24}$ J·T (electron dipole moment)
$d_p = 1.411 \times 10^{-26}$ J·T (proton dipole moment)
$r = 5.292 \times 10^{-11}$ m (radius of hydrogen atom)

$$F = \frac{3(1.257 \times 10^{-6})(9.285 \times 10^{-24})(1.411 \times 10^{-26})}{2\pi(5.292 \times 10^{-11})^4} = 1 \times 10^{-14}\ \text{N}.$$

Since this is the force exerted by two point magnetic dipoles that are oriented end to end, and whose separation is the radius of the hydrogen atom, this force will be reduced by a factor of ten to give a rough approximation of the downward (or upward) force on the electron shown in Fig. 2 for all dipole orientations encountered during a single orbit:

$$F_d = F/10 = 1 \times 10^{-15}\ \text{N} \qquad (14)$$

This will produce a torque on the orbiting electron:

$$\tau = F_d r = (1 \times 10^{-15})(5.292 \times 10^{-11}) = 5.292 \times 10^{-26}.$$

The angular momentum of the electron L_e is:

$$L_e = r_e m_e V_e = (5.292 \times 10^{-11})(9.109 \times 10^{-31})(2.188 \times 10^{6})$$

$$L_e = 1.055 \times 10^{-34}.$$

Note that $L_e = \hbar$, which cleaves to the rule that orbital angular momentum is confined to integer multiples of ħ, but it is smeared out to zero in the s shell due to induced magnetic dipole forces on the circular orbit that transforms it into a spherical orbit. Thus, orbital

angular momentum is never truly zero- it just gets smeared out to zero as the electron completes spherical orbits, or if it assumes a 90° angle with respect to an external magnetic field. The average rate of change Ω induced on the angle ϕ of the axis of the orbital angular momentum L_e of the orbiting electron can now be roughly estimated:

$$\Omega = d\phi/dt = \tau/L_e = (5.292 \times 10^{-26}) / (1.055 \times 10^{-34})$$

$$\Omega = 5.02 \times 10^{8} \text{ radians/second.}$$

The time t it takes for this axis to shift by 2π radians to trace out a spherical shell that will smear the orbital angular momentum out to zero is then:

$$t = 2\pi/\Omega \approx 1.25 \times 10^{-8} \text{ seconds}$$

With the electron completing 6.58 x 10^{15} orbits every second according to Equation (4), roughly 82 million orbits comprise each spherical shell, such that around 80 million spherical shells are being traced out every second, which smears the orbital angular momentum out to zero for the s shell. With the electron precessing 3.5 x 10^{11} complete rotations every second according to Equation (8), there are around 4,400 precession rotations for every spherical shell that is traced out. During that time, the proton has precessed around 6.6 complete rotations. In Fig. 3, the electron orbit has shifted by around ten degrees to produce a partial spherical shell. This works out to around 2 million electron orbits in 0.35 ns, during which time the electron has precessed around 120 complete rotations, while the proton has precessed only around 66 degrees.

No matter how many electron orbits it takes for them to be torqued into partial or complete spherical shells, taking the square root of the ratio between the number of orbits and the number of times the electron has precessed during that time will always result in the inverse fine structure constant 1/α. Perhaps the fine structure constant is calibrated to produce a predictable, recurring pattern of dipole interactions between the electron and the nucleus that results in the organized, repeatable generation of partial or complete spherical shells. Otherwise, electrons might orbit as disordered, nonuniform swarms from one atom to the next- even if the number of electrons were the same- that would not build up organized matter, and thus would make the emergence of life impossible.

This rough analysis confirms that electron precession could account for spherical electron orbits for the 1s orbital. Even if the magnetic force contributing to torque on elliptical orbits were weaker by yet another factor of ten (100 times weaker than point dipoles placed end to end), the electron would still trace out a spherical shell in 125 ns, and 8 million spherical shells would be traced out every second to smear the angular momentum out to zero. The values for higher order s orbitals can be similarly calculated, which will produce much lower rates of tracing out spherical shells. But, ultimately, more complex modeling is required that considers all the different electron orbits to establish whether the proposed source of the fine structure constant does indeed relate to the way two-dimensional elliptical orbits are transformed into three-dimensional spherical orbits. Now, if there are two or more electrons in a given orbital, the repulsion of their interacting electric fields would suffice to explain their elliptical orbits being jogged into three-dimensional orbits.

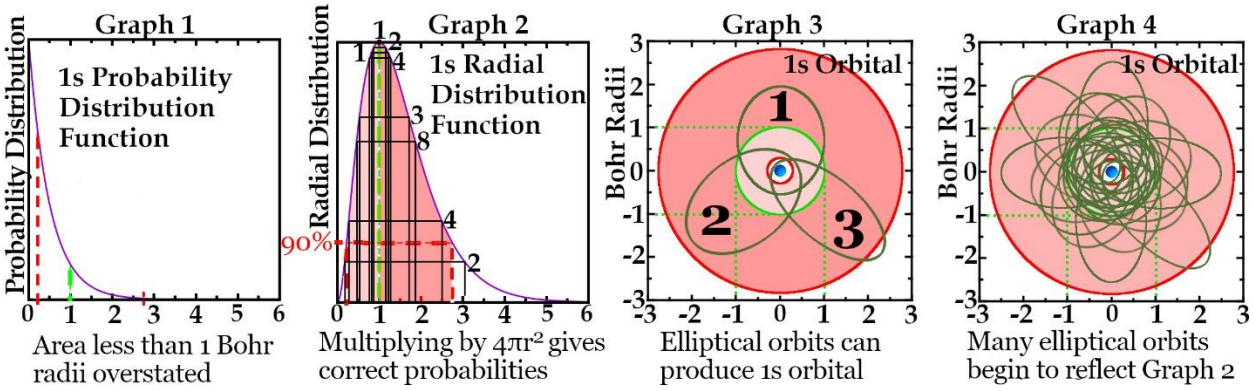

FIG. 4. Oscillating elliptical orbits in the 1s orbital can explain distribution functions. X-axes in Bohr radii.

Elliptical Orbits and the 1s Orbital

The probability distribution functions derived from Schrödinger's equation distort the most likely orbits for the electron. For example, the probability distribution for the electron in the 1s orbital labelled Graph 1 in Fig. 4 suggests that the electron spends the vast bulk of its time inside of one Bohr radius- the actual radius of the hydrogen atom owing to its orbiting electron. In fact, the electron would appear to have the highest probability of being within the nucleus! The dependency of the wavefunction on the orbital motion of the electron can be restored by considering concentric shells surrounding the nucleus such that the probability of finding the electron in different shells is what is plotted. This can be done by multiplying the wavefunction by the surface area of any given shell- $4\pi r^2$, which produces Graph 2. This is a radial distribution graph. The shaded regions represent 90% of the area under the curve where the probabilities are the highest. This corresponds to the electron being in the range of .25 to 2.75 Bohr radii of the proton, as seen by the projection of the red vertical dashed lines on the x-axis. The green dashed line shows that the maximum probability of finding the electron is now at the Bohr radius.

The novel derivation of the fine structure constant suggests that the electron is oscillating among different types of elliptical orbits due to magnetic dipole interactions with the proton. These are designated by the dark green ellipses labelled 1, 2 and 3 in the Graph 3 of Fig. 4. The most likely orbit is the light green circle that corresponds to one Bohr radius. In correlation with Graph 2, as areas within the red-shaded regions in the third graph get farther away from the green circle, there is a decreasing probability for the electron to be found in those areas. This simply means that there is a lower probability for the electron to assume more and more elongated elliptical orbits. Note that in Graph 2, the darker shaded portion (electron is more than 1 Bohr radius away from the proton) encompasses about twice as much area as the lighter shaded region (electron is closer than 1 Bohr radius), which indicates that there is around twice the probability of finding the electron outside of 1 Bohr orbit. This is entirely consistent with elliptical orbits in which the nucleus sits at one of the loci. Most of the elliptical orbit is outside of 1 Bohr orbit, so the electron spends more time there, and thus it has a higher probability of being found there.

All of the elliptical orbits to which the electron may oscillate are simulated by Graph 4 in Fig 4. Graph 4 selects 8 different elliptical shapes from a representative distribution based on the radial distribution function in Graph 2, where they are indicated by horizontal lines, along with the number of each elliptical shape selected. The point on the elliptical path where the electron is farthest from the proton corresponds to the right half of the radial distribution curve, and the point where the electron is closest to the proton for that elliptical shape corresponds to the left half of the curve. The ellipses in Graphs 3 and 4 have all been drawn fairly accurately with the nucleus placed at one of the loci.

A ring can be discerned in Graph 4 that is centered on 1 Bohr radius- precisely where the radial distribution curve gives the maximum probability for the electron's location. Thus, the novel derivation of the fine structure constant suggests that elliptical orbits cannot be peremptorily dismissed by saying that the electron exists in a superposition of states within an orbital that entirely ignores how the electron is moving; rather, the electron is moving in elliptical orbits, and the probabilities of finding it relate to capturing the orbit that it is in.

Fig. 5 shows the mechanism that may determine the eccentricity of the elliptical shapes for the electron orbits. Here, the electron is orbiting the proton in a horizontal elliptical path in one of the innumerable orientations the two particles can achieve through the interaction of their magnetic dipole moments while they are precessing. The 55-degree spin angles for the electron and proton may be

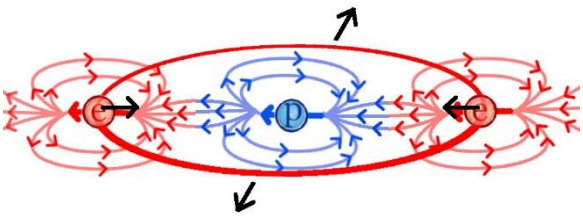

FIG 5. Magnetic Dipole effects on elliptical orbits. The eccentricity of the electron's elliptical orbit (red) in this orientation is being stretched into and out of the page due to forces imposed by the interacting magnetic dipole moments of the electron and proton

presumed to be into or out of the page for simplicity so that their dipole moments appear horizontal.

There will be a strong attraction between the magnetic dipole moments of the electron and proton near the left and right portions of the electron's path because the north pole of the proton (blue arrow) is end to end with the south pole of the electron, and vice versa. Midway between these areas, the magnetic field lines retain their orientations, and there will be a repulsion because the north pole of the electron (red arrow) is parallel and adjacent to the north pole of the proton. The black arrows indicate the forces that will increase the eccentricity of the elliptical path. All manner of eccentricities will result as the orientation of the electron's orbit constantly changes, and as the electron and proton precess on their spin axis.

Elliptical Orbits and Higher Energy Orbitals

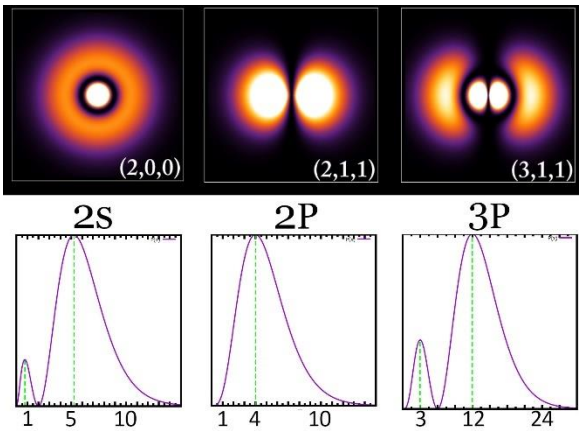

FIG. 6. Radial distribution curves for the 2s, 2p, and 3p orbitals. X-axis units are in Bohr radii. The 2p curve has a peak at the expected radius for an electron orbit, but no elliptical orbit can be visualized for p orbitals, which partially explains why electron orbits have been abandoned in favor of superposition- the electron's path has become irrelevant.

Fig. 6 shows radial distribution curves for higher energy orbitals for hydrogen. The first number in parenthesis in the upper row of orbital images denotes the shell (n), where the energy of a single electron is the same for all orbitals of that shell. The second number denotes the orbital angular momentum quantum number (ℓ), which historically proceeds according to increasing angular momentum in the sequence s, p, d, f, g, h, etc. The third number, the magnetic quantum number (m_ℓ), denotes the projection of the orbital angular momentum along a dimension of space in the presence of an external magnetic field. There are three possible configurations for any p orbital- the ones given in Fig. 6 are the $2p_x$ and $3p_x$ orbitals. According to Bohr theory, the expected radius r_n for a given shell n is determined from the formula $r_n = n^2 r_0$, where r_0 is the first Bohr orbit of the 1s orbital. Schrödinger's equation also produces this expected radius in terms of the highest probability for finding the electron there. The 2s and the 3p orbitals have two peaks on their radial distribution curves, which runs afoul of Bohr's theory. The single peak on the 2p curve at 4 Bohr radii conforms to Bohr theory ($2^2 r_0 = 4r_0$). This is where the centripetal force of the orbiting electron again matches the electrostatic force between the electron and proton, as it did with the 1s orbital. In fact, this will always be the case for the highest possible 'ℓ' value for a given shell. Thus, the 1s, 2p, 3d, 4f, 5g and 6h orbitals all have a peak in the radial distribution curve that matches Bohr's theory.

What might be causing two or more peaks in the 2s, 3p and other orbitals that do not match Bohr theory? These orbitals are farther away from the proton than at 1s, and thus, magnetic dipole interactions are weaker. The novel derivation of the fine structure constant may indicate that the electron is flipping between two or more orbits at different radii for orbitals that do not have the highest 'ℓ' value for a given shell that is farther out from the nucleus than the 1s shell. Here, torque on an elliptical orbit works towards completing a spherical orbit, but the orientation of the electron's spin axis with respect to that of the proton reaches a configuration that makes the orbit unstable due to weaker dipole interactions for the more distant orbital, which jolts the electron to an elliptical orbit in the inner radius. After working to complete a spherical orbit in the inner radius, a close pass with the proton would bring the electrostatic force into play for jolting the accelerated electron back into the outer orbit.

For example, the radial distribution curve for the 2p orbital in Fig. 6 has a single peak for the elliptical orbits. But the radial distribution curve for the more distant 3p orbital shows peaks for both an inner and outer orbit for the electron. Likewise, the radial distribution curve for the 2s orbital also shows peaks for an inner and outer orbit. The discussion from the previous section explains the rest of the area under the curve, as well as the volume of the orbitals, as the wandering of different orientations and eccentricities of elliptical orbits into which magnetic dipole interactions force the electron.

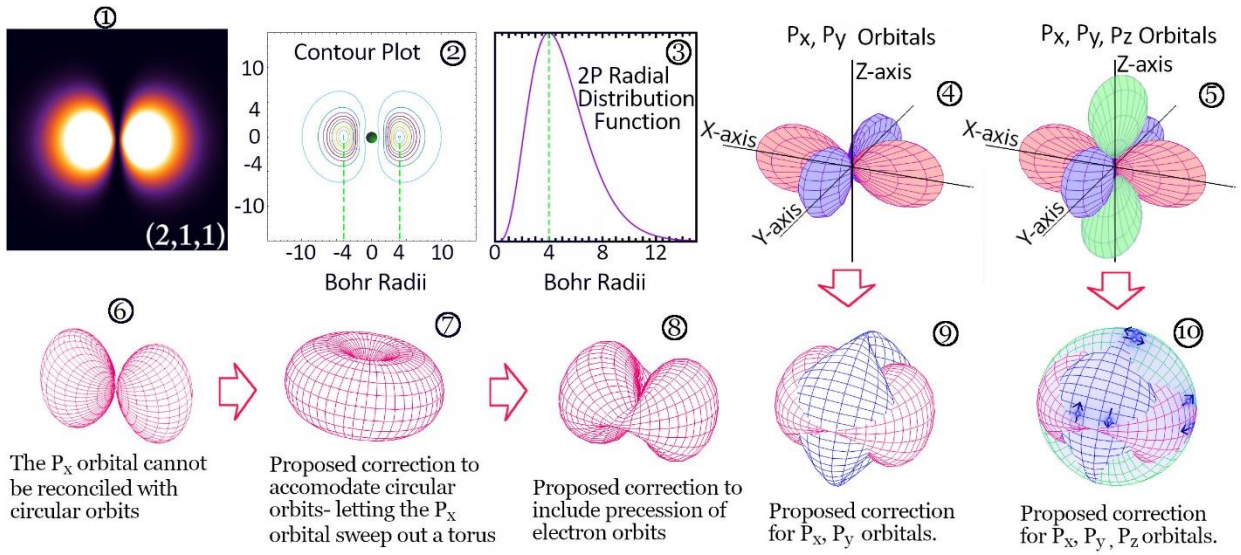

FIG. 7. The novel derivation of the fine structure constant applied to p orbitals. ① The P_x orbital according to quantum mechanics; ② Its contour plot; ③ Its matching radial distribution function; ④ Representation of the P_x, P_y orbitals- the four lobes correspond to the suggested modification below it to which the arrow points. ⑤ The P_x, P_y,, P_z orbitals- the six lobes correspond to the suggested modification below it. ⑥ The P_x orbital according to quantum mechanics; ⑦ Proposed correction; ⑧ Refined correction that considers precession of the orbiting electron to produce two lobes connected by flattened sections; ⑨ Proposed configuration for the modified P_x, P_y orbitals fit together. The flattened section of one orbital intrudes orthogonally into the wide section of the other orbital. ⑩ Proposed configuration for the modified P_x, P_y, P_z orbitals. The flattened sections of all orbitals intrude orthogonally into the wide sections of another orbital. Electron paths (blue arrows) might be highly synchronized- the atom might operate like a fine Swiss watch as partial or total spherical shells are being traced out in different orbitals.

The novel derivation of the fine structure constant suggests that a refinement might be needed with the way Schrödinger's equation is being manipulated to produce orbitals. The 2p orbital is the simplest starting point to show what this refinement might produce. Frame 1 in Fig. 7 shows the two lobes of the $2p_x$ orbital. No elliptical orbit can possibly be visualized with these two disconnected lobes. It becomes quite whimsical attempting to explain how an electron can get from one lobe to another when there is zero probability for the electron to be in the space between the two lobes. Since such an exercise conjures up similarities with attempting to explain how a single electron can go through two slits simultaneously in the two-slit experiment, elliptical orbits were readily dismissed in favor of superposition, in which the electron's path became irrelevant- as with the two-slit experiment, the path of the electron was swallowed up by its wavefunction. But to reiterate, this paper proposes that collapsing the wavefunction to reveal the electron's location amounts to capturing it in a particular orbit. As such, there cannot be a gap between the lobes of an orbital where the probability of finding an electron is zero. It only remains to propose a correction to the orbitals produced by Schrödinger's equation where, at present, no elliptical path can be visualized due to gaps between lobes.

The fact that the contour plot and the radial distribution curve for any 2p orbital (Fig. 7 Frames 2, 3) still reproduce the most likely orbit of 4 Bohr radii for the electron should have been a hint that elliptical orbits may have been dismissed a little too hastily. The contour plot of Fig. 7 Frame 2 is a more detailed version of the orbital shown in Frame 1. The contour plot shows a sequence of concentric outlines, in which each outline, or contour, represents the same probability of finding the electron. The highest probability of finding the electron near the center of both lobes corresponds to the radius of an orbit in which the centripetal force again is equal to the electrostatic attraction. Since the inability for an electron to traverse the gap between the lobes presents an insurmountable obstacle to such an orbit, it may be worthwhile to entertain the notion that the two lobes might be inappropriately carved-out volumes of a torus in which elliptical orbits are possible, as shown by the progression from Frame 6 to Frame 7 in Fig. 7.

But the two lobes derived by throwing all manner of substitutions and arcane mathematical tricks at Schrödinger's equation have proven amenable for

explaining many chemical reactions. With the novel derivation of the fine structure constant suggesting that elliptical orbits are being torqued into spherical orbits through dipole interactions, the progression from Frame 7 to Frame 8 of Fig. 7 can be conjectured for the P_x orbital, which will retain much of the profile of two distinct lobes. In Frame 8, the torus has been flattened in two areas that are 180° apart. Fig. 8 depicts an enlarged view of the P_x orbital, with a head-on view of the flattened section shown below it, which is identical to the P_x orbital produced by Schrödinger's equation (Fig. 7 Frame 1), except for the thin connection between the two lobes that is conspicuous in the top image of Fig. 8. An electron can now freely travel between the two lobes to complete elliptical orbits.

The image of the dual-lobed torus has been generated by Gnuplot. The code to produce the image may be a guide to how Schrödinger's equation should be manipulated to accommodate torqued electron orbits that are suggested by the novel derivation of the fine structure constant. The crucial lines of code are:

```
set parametric
set urange[-pi:pi]
set vrange[-pi:pi]
        ⋮
set xrange [-2:2]
set yrange [-2:2]
set zrange [-18:18]
splot cos(u)+1.0*cos(u)*cos(v)\
, sin(u)+ 1.0*sin(u)*cos(v)\
, abs(u)*abs(u+pi)*abs(u-pi)*sin(v).
```

To generate the torus in Frame 7 of Fig. 7, the final line of the code, which controls the z-axis, only requires the single term 'sin(v)'. When this term is multiplied by the three absolute value terms 'abs(u)*abs(u+pi)*abs(u-pi)', the dual-lobed torus with flattened sections 180° apart is generated. The absolute value terms establish a line of zero-crossings of the XY plane that bisect the torus vertically as gnuplot is processing the values in 'urange' and 'vrange' from lines 2 and 3 of the code above. These zero crossings do not indicate zero probability for the electron's location in these points. These are valid points defined by the zero-crossing line at which an electron can cross from one lobe to another. As will be shown, the zero-crossing line acts as a pivot around which different elliptical orbits may tilt to trace out a partial spherical shell.

Frame 4 of Fig. 7 shows the P_x and P_y orbitals as derived by Schrödinger's equation. Frame 9 below it proposes a modification to the way they fit together. The aspect of two lobes is retained in both the P_x and P_y orbitals by having the flat sections of one torus intrude into the thick portions of the other torus. Frame 10 shows how all three p orbitals would fit together in this scheme. Rather than random positions for the electrons, the atom may function like a highly synchronized Swiss watch. For example, in completely filled P_x, P_y, P_z orbitals, the total angular momentum is zero. The opposite spins of paired electrons in each dual-lobed torus cancel, and they orbit in opposite directions in each dual-lobed torus so that the angular momentum is cancelled. The electrons in any given orbital would cross one another in the wide sections of the toruses, with all electrons

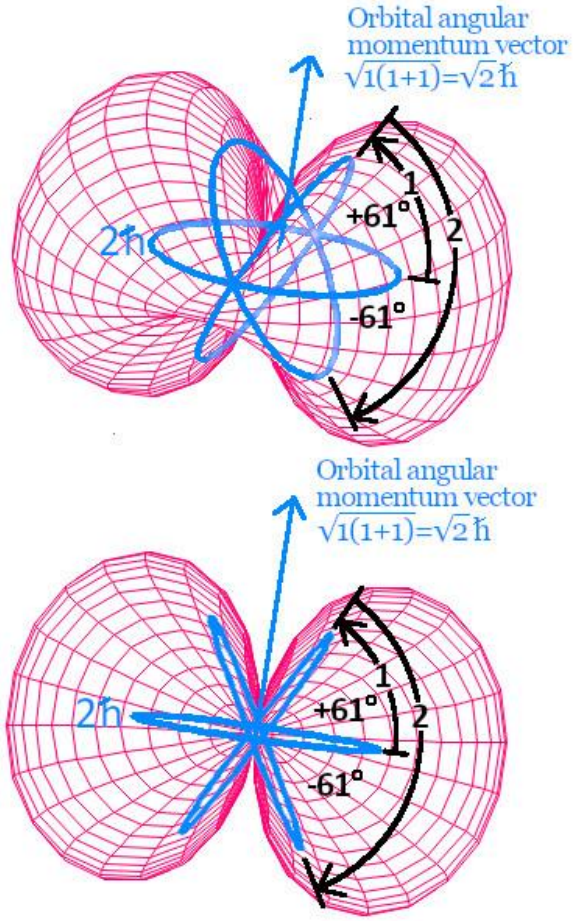

FIG. 8 Top: The novel derivation of the fine structure constant applied to p orbitals. Bottom: A view directly at the flattened section of the torus is identical to the p orbitals produced by Schrödinger's equation, with the exception of a bridge of nonzero thickness between them. The incomplete spherical shell traced out by electron orbits being torqued to ± 61° smears their angular momentum of 2ħ to √2ħ.

present in the wide sections of their respective orbital at that time, as shown in frame 10. All the electrons would then proceed in their orbit so that they would all arrive in the thin sections, but now any two electrons in a given orbital would be 180° apart.

As mentioned, the flat sections serve as a pivot line for elliptical orbits being torqued into spherical orbits. This is illustrated in Fig. 8. According to Bohr theory, the orbital angular momentum of an orbiting electron is L=nħ. For the 2p orbital, where n=2 and ℓ=1, Bohr theory predicts L=2ħ for an electron orbiting at 4 Bohr radii, whereas Schrödinger's equation predicts L=$\sqrt{\ell(\ell+1)}$ħ=√2ħ for the orbital. Meanwhile, the 2s orbital, with ℓ=0, again winds up with L=0ħ according to manipulations on Schrödinger's equation, whereas the novel derivation of the fine structure constant suggests that s orbitals are being smeared to zero angular momentum by elliptical orbits being torqued into spherical ones.

The novel derivation of the fine structure constant can also be brought to bear on p orbitals to reconcile Bohr theory with Schrödinger's equation. Fig. 8 shows an electron orbiting at 4 Bohr radii within the p orbital, with an angular momentum of 2ħ. The arc labelled '1' represents magnetic dipole interactions between the electron and proton producing torque to trace out a spherical shell. But because the electron is farther away from the proton in the 2p orbital, the electron arrives at an orientation and precession angle with the proton where magnetic dipole interactions weaken. At a tilt angle of +61°, the torque reverses to trace out the arc labelled '2'. As the tilt angle approaches -61°, the torque again weakens, and then reverses to repeat the process. Only a partial spherical shell is traced out, which smears the angular momentum of 2ħ for a single electron orbit to √2ħ, according to Schrödinger's equation. But only integral multiples of 1ħ for angular momentum can be detected in our three-dimensional universe. In the presence of an external magnetic field, the partial spherical shell assumes an angle that will force 1ħ to become manifest as a component of √2ħ along the direction of the magnetic field. Where the electron assumed a spin angle of 55° in the presence of a magnetic field, the p orbital assumes an angle of either 45° or 90° to produce 1ħ or 0ħ, respectively, so that the magnetic quantum number (m_ℓ) is 1 or 0.

In effect, the formula derived from Schrödinger's equation, L=$\sqrt{\ell(\ell+1)}$ħ, is essentially a smearing factor that reduces the angular momentum nħ of a single electron orbit as it is being torqued into a spherical shell by magnetic dipole interactions between the electron and the proton, as suggested by the novel derivation of the fine structure constant. For the s shell, the smearing factor reduces the angular momentum to zero as a complete 360° shell is traced out. For the p shell, only a 122° shell is traced out- the angular momentum is not smeared out to zero. For the d, f and higher order shells, the electron is farther and farther away from the proton, and dipole interactions become weaker and weaker- the torque peters out earlier to produce smaller and smaller partial shells. The smearing factor L=$\sqrt{\ell(\ell+1)}$ħ approaches L=nħ for the largest ℓ value in a higher order shell- the angular momentum of a single electron orbit. For lower ℓ values in higher order shells, the electron is toggling between two or more orbits. As with the s orbital, the expanse of the p orbital simply defines the extent of eccentricity of elliptical orbits. If an electron is located near the outer perimeter of one lobe, its orbit has an extreme eccentricity that will carry it near the inner perimeter of the other lobe close to where the two lobes are bridged.

The ±61° angle through which electron orbits are torqued into partial spherical shells for 2p orbitals has been derived by setting the average value for the angular momentum vector in Fig. 8 equal to √2ħ, given that the angular momentum for an orbiting electron at 4 Bohr Radii is 2ħ. The equation for finding the average value of a function is:

$$\frac{1}{b-a}\int_a^b f(x)dx,$$

where the integration of f(x)=2ħcos(x) will give the average magnitude of the component of the orbiting electron's angular momentum in the direction of the angular momentum vector in Fig 8.

By symmetry, the value of the orbital angular momentum vector in Fig. 8 in that orientation will be the same whether electron orbits are torqued from +61° to -61°, or from the horizontal position at the starting position of 0° for arc 1 to the terminal position at +61°. So, a=0 and b=61° will be used in the equation above. Since the torque wanes as ±61° is approached, the electron spends more time orbiting near those orientation angles, and moves through the horizontal position more rapidly. This must be considered in finding the average value; otherwise it will be overstated. Thus, simple harmonic motion (SHM) will be applied to the shifting of the electron orbits to produce a partial spherical shell. The range

of the SHM will be taken from a=0° to b=+61°, where 'b' will now be the unknown variable (in radians) whose value is to be determined. The SHM function is then:

$$\cos\left[\frac{\pi}{2b}\right]\theta.$$

The function will be at a maximum at θ=0, and a minimum at θ=b. The magnitude of the velocity of the SHM function is:

$$\left|\frac{d}{d\theta}\cos\left[\frac{\pi}{2b}\right]\theta\right| = \left|-\frac{\pi}{2b}\sin\left[\frac{\pi}{2b}\right]\theta\right| = \frac{\pi}{2b}\sin\left[\frac{\pi}{2b}\right]\theta$$

This function will be at a maximum at θ=b, and a minimum at θ=0, which will emphasize the angles near 'b' where the electron orbits within the p orbital linger longer, and deemphasize the angles near the horizontal position where the orbits shift more rapidly. This SHM velocity function will modulate the f(x)=2ħcos(x) function for the angular momentum by multiplying it. The angle derived for 'b' can only be considered an estimate because the SHM velocity function may not be the most refined way to deal with the way electron orbits are being shifted at varying rates- much more complex modeling with precessing magnetic dipoles is required. So, this derivation is an initial, tentative attempt to determine the extent of the partial spherical shell traced out by orbiting electrons in the p orbital to within a few degrees. The average value function is then:

$$\frac{1}{b-a}\int_a^b f(x)dx = \frac{1}{b}\int_0^b \left[\frac{\pi}{2b}\sin\left(\frac{\pi}{2b}\right)\theta\right] 2\hbar\cos\theta\, d\theta = \sqrt{2}\hbar$$

The coefficient '2ħ' in front of the cosine function represents the angular momentum of an electron orbiting at 4 Bohr Radii for the p orbital. The average value of the angular momentum as the orbit traces out a partial spherical shell has been set to √2ħ, as predicted by $L=\sqrt{\ell(\ell+1)}\hbar = \sqrt{1(1+1)}\hbar = \sqrt{2}\hbar$. The equation will be solved for 'b'- the maximum angle of the tilted electron orbits as a partial spherical shell is traced out.

The first step is use half-angle formulas to simplify the integration, with 'ħ' cancelling from both sides:

$$\frac{1}{b}\int_0^b \frac{\pi}{2b}(2)\left(\frac{1}{2}\right)\left\{\left[\sin\left(\frac{\pi}{2b}+1\right)\theta\right]+\left[\sin\left(\frac{\pi}{2b}-1\right)\theta\right]\right\} d\theta = \sqrt{2}$$

$$= \frac{\pi}{2b^2}\int_0^b \left\{\left[\sin\left(\frac{\pi}{2b}+1\right)\theta\right]+\left[\sin\left(\frac{\pi}{2b}-1\right)\theta\right]\right\} d\theta$$

$$= \frac{\pi}{2b^2}\left[\frac{-1}{\pi/_{2b}+1}\cos\left(\frac{\pi}{2b}+1\right)\theta - \frac{1}{\pi/_{2b}-1}\cos\left(\frac{\pi}{2b}-1\right)\theta\right]_0^b$$

$$= \frac{\pi}{2b^2}\left[\frac{-1}{\pi/_{2b}+1}\cos\left(\frac{\pi}{2}+b\right) - \frac{1}{\pi/_{2b}-1}\cos\left(\frac{\pi}{2}-b\right) + \frac{1}{\pi/_{2b}+1} + \frac{1}{\pi/_{2b}-1}\right]$$

$$= \frac{\pi}{2b^2}\left[\frac{\sin b}{\pi/_{2b}+1} - \frac{\sin b}{\pi/_{2b}-1} + \frac{1}{\pi/_{2b}+1} + \frac{1}{\pi/_{2b}-1}\right]$$

$$= \frac{\pi}{2b^2}\left[\frac{\sin(b)+1}{\pi/_{2b}+1} - \frac{\sin(b)-1}{\pi/_{2b}-1}\right]$$

$$= \frac{\sin(b)+1}{b+2b^2/_{\pi}} - \frac{\sin(b)-1}{b-2b^2/_{\pi}} = \sqrt{2} = 1.414$$

b=1.065 radians = 61° is the graphical solution.

So, the magnitude of the orbital angular momentum vector shown in Fig . 8 will be √2ħ=1.414ħ when electron orbits with a magnitude of 2ħ are swept through an angle of ±61° to trace out a partial spherical shell for the p orbital. Without considering SHM, the magnitude would be 1.64ħ for a sweep angle of ±61°, which overstates 1.414ħ by 16%. And if the sweep angle were derived without considering SHM, it would be ±79.7°. So, a sweep angle of ±61° is an entirely reasonable estimate in considering the waning, and then reversing torque on electron orbits as the terminal angle is approached. Moreover, a sweep angle of ±61° conforms nicely to the maximum extent of the contours of the dual-lobed torus presented in Fig. 8 that can be taken to represent the volume within which there is a 99% probability of finding the electron.

Thus far, the novel derivation of the fine structure constant has been applied to a single electron occupying a p orbital, in which the orbital angular momentum is 1ħ- the average angular momentum vector of the partial spherical shell (√2ħ) assumes an angle of 45° in the presence of an external magnetic field, which entails the p orbital orienting itself at 45°. The spin angular momentum of the electron (1/2ħ) is opposite to its orbital angular momentum, which results in a total angular momentum of 1/2ħ. As mentioned, when the P_x, P_y, P_z orbitals are filled with six electrons, the total angular momentum is zero, owing to the opposite spins of paired electrons in each orbital cancelling, and the opposite orbits in

each orbital cancelling. The novel derivation of the fine structure constant must account for the total angular momentum of any number of electrons in the p orbitals. The spins, orbital angular momenta and total angular momenta of atoms is designated by $^{2S+1}L_J$, where 'S' is the total spin, 'L' is the total orbital angular momentum given in the s, p, d convention, and 'j' is the total angular momentum consisting of both spin and orbital motion. The angular momenta of the p orbitals are designated as follows:

$P^1 = {}^2P_{1/2}$	$P^3 = {}^4S_{3/2}$	$P^5 = {}^2P_{3/2}$
$P^2 = {}^3P_0$	$P^4 = {}^3P_2$	$P^6 = {}^1S_0$

These angular momenta values are identical regardless of the shell- 2p, 3p, 4p, etc. Thus, the total spins and total angular momenta of the carbon atom $(2p)^2$ are identical to those of silicon $(3p)^2$ and germanium $(4p)^2$. The p^1 (one electron present in the p orbitals) and p^6 (p orbitals fully filled with six electrons) configurations have already been characterized. For p^5, the unpaired electron has a spin of ½ħ- thus 2S+1=2 for the superscript. Four of the electrons fill two p orbitals, and each pair of electrons in the filled orbitals are orbiting in opposite directions. This leaves the unpaired electron in the third orbital with an orbital angular momentum of 1ħ, which is designated by the 'P'. The total angular momentum of 3/2 (spin and orbital motion) in the subscript indicates that the unpaired electron is spinning in the same direction in which it is orbiting. This is in contrast with the p^1 orbital, where the lone electron is spinning in an opposite direction from its orbit. These orientations have been characterized by Hund's rules.

The orbital angular momenta of the P^2, P^3 and P^4 orbitals clearly suggest electron orbits that are tilted with respect to one another. Otherwise, how can the two electrons of the P^2 configuration produce an angular momentum of 1ħ, or the three electrons of the P^3 configuration produce 0ħ? The novel derivation of the fine structure constant guides the way to a resolution. The middle diagram of Fig. 9 reproduces the dual-lobed toruses of the three p orbitals fit

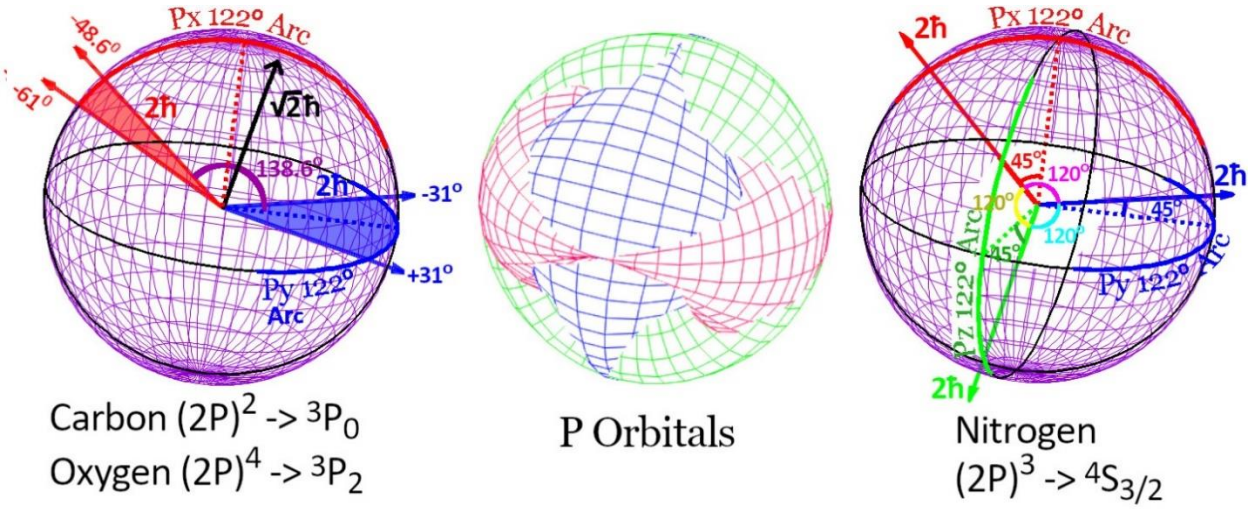

FIG. 9. Explaining the angular momenta of p orbitals in terms of the novel derivation of the fine structure constant. Center image: the three dual-lobed toruses of the P_x, $P_{y,}$, P_z orbitals. Right image: the colored arcs represent the oscillating, 122° paths of the angular momentum vectors traced out by each p orbital of matching color, with the midpoints of the arcs corresponding with the middle electron orbit depicted in Fig. 8 that starts arc 1. For nitrogen, the three electrons are locked into distinct elliptical orbits whose angular momentum vectors are offset 45° from the center position of the arcs they otherwise would trace out. This establishes 120° between the vectors to cancel the orbital angular momentum to zero. Left image: the elliptical orbits of the two outer electrons of carbon in two different p orbitals are locked into the range of oscillation indicated to maintain an angle of 138° between their angular momentum vectors. With each elliptical orbit producing an angular momentum of 2ħ, the 138° angle between the two vectors results in an average orbital angular momentum of √2ħ, whose vector assumes an angle of 45° in the presence of an external magnetic field to produce 1ħ, which rotates the two p orbitals accordingly. For oxygen, there is a filled p orbital whose two electrons orbit in opposite directions so that their angular momenta cancel. The orbital angular momentum vectors of the remaining two electrons in two different p orbitals assume the range of oscillation shown that is identical to carbon.

together. This will assist with visualizing the angular momentum vectors that are traced out due to interacting dipole moments between the electrons and the nucleus that torque elliptical orbits into partial spherical shells according to Fig. 8.

The right image of Fig. 9 shows the paths of all three angular momentum vectors as 122° arcs (±61° sweep angles), whose colors matches the colors of the dual-lobed toruses in the middle diagram that generate them. Dashed lines indicate the midpoints of the 122° arcs, which represent the middle orbit that starts arc 1 in Fig. 8. The right image of Fig. 9 proposes a resolution to the $^4S_{3/2}$ state of the p^3 configuration, in which the 'S' designates zero total orbital angular momentum. The only way to get three equal vectors to cancel is if they are oriented at 120° from one another in the same plane. This orientation will be achieved if the orbital angular momentum vectors generated by each of the three orbiting electrons is offset 45° from the midpoint of each arc, as shown.

For the p^3 configuration, there is a lone electron in each P_x, P_y and P_z orbital whose angular momentum vectors are ordinarily capable of tracing out a 122° arc as their elliptical orbits are torqued into partial spherical shells. But in the p^3 configuration, each elliptical orbit is fixed in a plane whose orbital angular momentum vector forms an angle of 120° with the vectors of the other two orbiting electrons. The constraint of limiting the orbital angular momentum that is manifest in our three-dimensional universe to integral multiple of ħ overwhelms the torquing force that transforms elliptical orbits into spherical orbits. But the eccentricities of the elliptical orbits can all change simultaneously, as long as the total orbital angular momentum cancels out to zero. With the orbital angular momentum being zero (S), the spins of the three electrons are all parallel to produce a total spin of 3/2 in the subscript, and 2(3/2)+1=4 for the superscript.

It only remains to invoke the novel derivation of the fine structure constant to resolve the p^2 and p^4 configurations. The p^2 configuration has two electrons in two different p orbitals, given as P_x and P_y in the left image of Fig. 9. The p^4 configuration has one p orbital filled with two electrons, whose opposite orbits and spins cancel their total angular momentum to zero. The remaining two electrons are in two different orbitals, which results in the same situation as the p^2 configuration. If the orbital angular momentum vectors of the two unpaired electrons in the p^2 and p^4 configuration are 138.6° apart, their magnitudes of 2ħ will combine to produce √2ħ, whose vector will again assume an angle of 45° in the presence of an external magnetic field to manifest as 1ħ in our three-dimensional universe- the p orbitals will wind up orienting themselves at a 45° angle as they take the vector with them.

The 138.6° angle is readily derived by applying the law of cosines to a triangle with two legs of length 2ħ, and the third leg of length √2ħ. The orbital angular momentum vectors for the two electrons are 138.6° apart if the one for the P_y electron points at the midpoint of its arc, and the one for the P_x electron is offset -48.6° from its midpoint. Spherical coordinates will show that P_x can then stray to its limit of -61°, while P_y can stray to either +31° or -31° in a nonlinear fashion to maintain 138.6° between the two vectors. With the total orbital angular momentum assuming 1ħ (P) along one dimension of space, the two unpaired electrons in two different p orbitals have parallel spins to produce 2(1)+1=3 in the superscript. For p^2, the spins are opposite to the orbital angular momentum to yield 0 for the subscript; while the spins and orbital angular momentum are in the same direction for p^4 to yield 2 in the subscript.

Conclusion

Schrödinger's equation yielded a number of important, seminal insights into the behavior of the quantum world, and it corrects several false results of Bohr theory. But the novel derivation of the fine structure constant suggests that spin precession is a mechanism that has been leapfrogged in manipulating Schrödinger's equation to produce electron orbitals. This paper has proposed that the integration of this mechanism entails preserving elliptical orbits for the electron in deriving the shapes of orbitals. The 1s orbital can be explained by imposing its radial distribution curve on various eccentricities of elliptical orbits. Higher energy s orbitals, as well as orbitals with more than one peak in their radial distribution curve, may involve the elliptical path of the electron being jolted into different radial orbits. Because s orbitals trace out complete shells, their orbital angular momentum is smeared out to zero. P orbitals, with angular momentum L=√2ħ, as well as orbitals with greater angular momentum, may require an adjustment to their shapes. This paper has proposed that their cross-sections may actually be those of dual-lobed toruses. The spin and orbital angular momenta of all

the p configurations have been explained in terms of the novel derivation of the fine structure constant that implies that elliptical orbits are being torqued into partial spherical orbits through dipole interactions between electrons and the nucleus. The d, f and higher order orbitals should likewise be amenable to being explained by bringing the novel derivation of the fine structure constant into play.

This derivation has been referred to as "novel" in this paper simply because it is unique and new, but it may be the true source of the fine structure constant: $1/\alpha=\sqrt{f_e/f_L}=137$. The ratio between f_e (the rotation rate of the electron in the first Bohr orbit) and f_L (the Larmor precession rate of the electron in the first Bohr orbit) is the relationship that permits electrons to orbit nuclei in repeatable, organized patterns. The inverse of this ratio (α) is found in a variety of equations that describe the quantum world, as is the square root of this ratio as well as other powers of α.

The fine structure constant has fascinated physicists because it implies the existence of consciousness that predates the Big Bang, in which the most crucial constants of physics appear to have been fine-tuned to permit life to emerge. The novel derivation of the fine structure constant suggests that establishing a precise ratio between the precession rate of electrons and their rotation rate around the nucleus to torque elliptical orbits into spherical ones through dipole interactions is a key consideration for allowing atoms to assume organized, repeatable patterns of electrons to enable chemical reactions to proceed in a consistent manner that would lead to the construction of biomolecules. Otherwise, there might be disorganized swarms of electrons in which atoms with the same number of electrons undergo dissimilar, random chemical reactions to build up matter in a haphazard fashion that would make the emergence of life impossible.

Once the value of the fine structure constant is set to enable electrons to assume organized, repeatable patterns of spherical orbits around nuclei, atoms may operate like fine Swiss watches. Partial or complete spherical shells may be traced out in all the orbitals in a highly synchronized manner, with electrons passing one another in a precisely timed scheme. Quantum mechanics may be retracing the deliberations and steps of pre-Big Bang consciousness in dealing with the intricacies and complications of opening up three-dimensions of space into which life can be made to emerge, where before there may only have been one or more dimensions of time. But, as the novel derivation of the fine structure constant suggests, quantum mechanics has missed a few steps.

While the proposed source of the fine structure constant can fully explain orbitals, why are they also manifest as wavefunctions? Having tweaked the crucial constants of physics that determine the value of the fine structure constant so that repeatable organized atoms will permit life to emerge, the atoms can be left to run on their own- their wavefunctions take over. The two electrons of any one of the three p orbitals are proposed in this paper to cross one another in the wide portions of the dual-lobed torus in operating like the components of a fine Swiss watch, whereas only a single electron is ever present in one of the thin portions. Thus, there is twice the probability of finding an electron somewhere in one of the wide portions while electrons are crossing there. Furthermore, the electron can only cross the lobes along a line of near-zero thickness. This may have the effect of the wavefunction deemphasizing the thin portions to the extent that two separate lobes result in the way that p orbitals are derived from Schrödinger's equation.

The novel derivation of the fine structure constant may then only apply to orbitals once their wavefunction has collapsed, which reveals electrons operating like the components of a fine, highly synchronized Swiss watch. A variety of ideas about how the wavefunction and its collapse relate to reality have been proposed, such as the Copenhagen interpretation and the many-worlds interpretation. The basic premise of the Copenhagen interpretation is that all reality is essentially in an undefined state- a wavefunction- until it is observed. The moon, for example, does not exist until you look at it, which collapses its wavefunction. The many-worlds interpretations holds that there are a near-infinite number of universes in coexistence that diverge with each wavefunction collapse. The role of consciousness is paramount in the Copenhagen interpretation, and rendered insignificant in the many-worlds interpretation.

Since the novel derivation of the fine structure constant strongly implies that it was fine-tuned by pre-Big Bang consciousness before any universe came into existence, the many-worlds interpretation- which would have to include universes where the fine structure constant had many different values- is ruled out. Indeed, it would be quite dejecting for pre-Big Bang consciousness to have managed to devise a three-dimensional universe that permitted life to emerge after an undoubtedly gargantuan and unimaginably complex effort, when a lab assistant can

cause a new universe to become manifest simply by flipping a switch on a tabletop lab experiment that permits detecting which of two slits an electron went through.

The novel derivation of the fine structure constant leads to yet another proposal for reconciling wavefunctions with reality. Once life emerges, only those aspects of our three-dimensional universe that are directly perceptible to life need to have their wavefunctions collapsed. There are inadequate conscious resources available to pre-Big Bang consciousness for collapsing the wavefunctions of all the quantum particles in our universe. The vast bulk of them will never be detected by the consciousness that is projected to life anyway, so they can remain as wavefunctions. These intact wavefunctions can then be likened to subconscious processes- they only intrude into consciousness when absolutely necessary, otherwise, consciousness becomes overloaded and disordered.

As an everyday example of a subconscious process intruding into consciousness, one might feel an unusual sense of something special associated with a store sign that was passed while driving a car through town. After a few seconds of struggling to discern the significance, a memory is sparked of having researched the internet a few weeks before for a product that was needed- it was only available at that store. The Copenhagen interpretation would allow for two outcomes. The driver decides to execute one them by making a U-turn and parking in the store's parking lot to purchase the product. A new universe would not have become manifest if the driver had failed to recall the memory of researching the internet and had executed the other outcome of continuing to drive through town. Subconscious processes determined the greater part of that outcome, not conscious ones. Whether conscious processes and/or unconscious processes in living creatures are somehow linked with pre-Big Bang consciousness to cause wavefunction collapse is an intractable question far beyond what can be tested, since not the slightest progress has been made in characterizing the origin of consciousness itself.

All that can be done is to grope for phenomena that characterize the origin of tangible things and apply them to consciousness. Since a successful theory often explains and connects various, seemingly unrelated mysteries, a theory of the origin of consciousness might show promise if it exhibits this trait. In our universe, tangible things originate as opposite pairs. A positron will always accompany an electron when it emerges from a high energy photon; an antiproton will always accompany a proton; and an antineutron will always accompany a neutron. Does consciousness originate as an opposite pair? Such a premise would connect a variety of seemingly unrelated mysteries. It would explain the coexistence of the opposite forces of love and evil that humans have always been deeply familiar with, but that have been mischaracterized as good and evil- "good" is too general a term to apply to the modulation of consciousness that "evil" or "love" refer to directly in their polar opposite effects. The emergence of consciousness as an opposite pair would also explain the coexistence of two brain hemispheres in all evolved living creatures that operate as separate systems- the elucidation of which has otherwise thus far been entirely inadequate. Since consciousness cannot be found in the brain, each of the two brains must function as a sort of transceiver between life and consciousness.

It seems that once life has been made to emerge by forcing electrons to assume repeatable, organized patterns around nuclei through the precise calibration of the fine structure constant, the opposite twins that become manifest as a condition of the origin of consciousness must both be separately accommodated when they are projected to brains to experience an equal share in the new mode of existence. Thus is explained the duality of man- equally capable of acts of love and acts of evil. And thus is resolved the philosophical and religious conundrum of why an omnipotent "god" of love permits evil on our planet.

Love and evil are the equal, countervailing forces that constitute the emergence of consciousness as an opposite pair- a theory that shows promise by fulfilling the condition of resolving a variety of other mysteries. This theory might represent the first, real progress in explaining consciousness, as well as the motivation behind the construction of our three-dimensional universe as an escape from the undoubtedly sensory-deprived regime where consciousness emerged as an opposite pair under constant threat of mutually annihilation- like particle-antiparticle pairs. The novel derivation of the fine structure constant that fine-tuned the properties of the most crucial constants of physics to permit electrons to orbit in organized, repeatable patterns in order for life to emerge would then have been the key to engineering the escape.